1. Physical Status and Analytical Decomposition

ΔLP is proposed as a kinematic diagnostic index that serves as a proxy for radiative redistribution. Expressed in kilometers (km), this metric quantifies lateral geometric variations across interannual to decadal scales. Rather than acting as a standalone forcing term, ΔLP captures the interannual geometric reconfiguration of the Earth-Sun vector, providing a measurable link between orbital dynamics and planetary energy distribution.

The analytical decomposition $LP = D\_au \cdot \sin(\delta)$ reveals that the observed displacement of ≈ 360,000 km (2000–2025) is the combined result of radial distance (D_au) and solar declination (δ). In this relationship, D_au acts as a positional factor within the orbital band that scales and amplifies subtle variations, while δ defines the magnitude of change in the lateral vector. This coherent coupling supports the proposed Relative Geoenergetic Equilibrium (RGE) Hypothesis (See Figure 1: *Orbital Window Proxy Scale*).

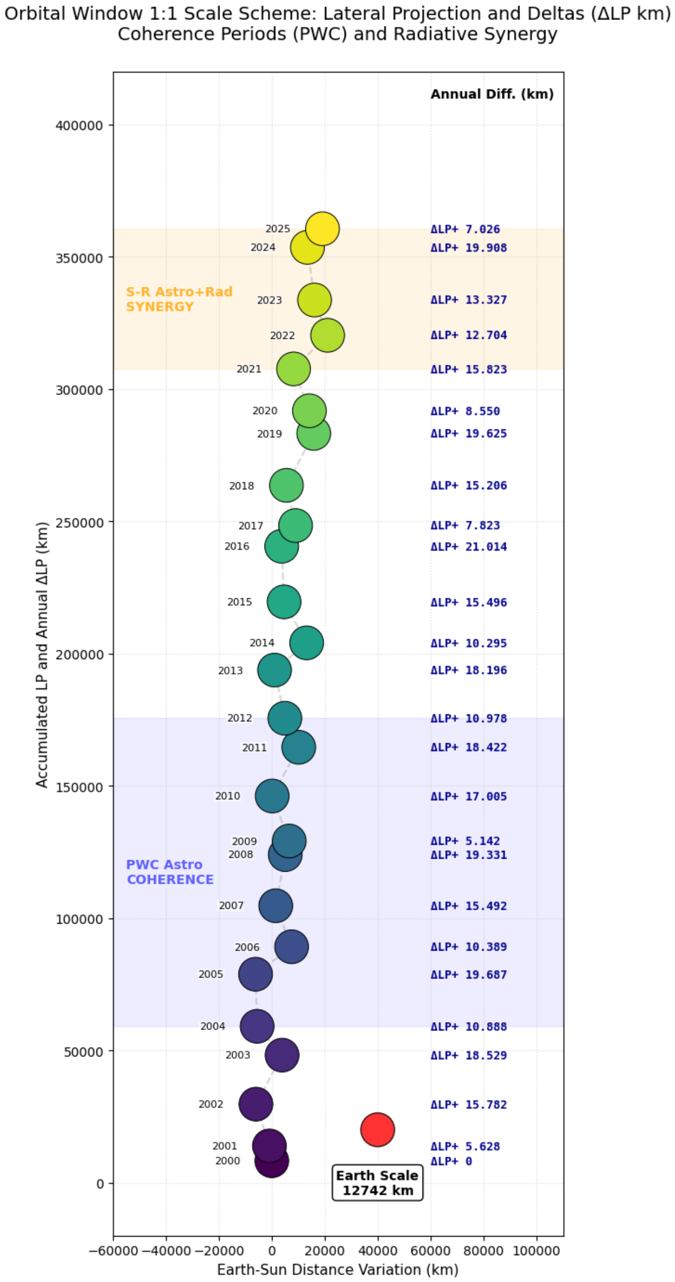

Figure 1 Proxy Scale orbital window scheme: lateral projection (LP) and annual deltas (2000–2025). Earth spheres (d_E ≈ 12,742 km) are plotted by radial distance variation and cumulative lateral displacement. Shaded areas indicate statistical regimes from PWC/MWC: Astro Coherence (2004–2012) and Astro-Radiative Synergy (S-R) (2021–2025). High ΔLP values (e.g., +19,908 km in 2024) correlate with structured radiative anomalies, supporting ΔLP as a kinematic proxy for global energy redistribution and the RGE Hypothesis.

2. Radiative Mapping and Information Theory

Although the cumulative series reaches 360,000 km, the Information Theory analyses (PWC/MWC) utilize interannual differences (ΔLP). These values were integrated with the BEST climate index and CERES TOA (incoming flux) radiation data. Geometrically, this displacement modulates the latitudinal distribution of the solar zenith angle, directly affecting radiative gradients over the oceans, particularly at critical latitudes such as 45.5° S and 45.5° N.

The high statistical coherence found through PWC/MWC suggests a structured association, where the kinematic state of the orbit preconditions the radiative budget. This reinforces the use of ΔLP as an innovative diagnostic tool for astro-climatic coupling.

3. Coherence Periods and Climate Dynamics

High-coherence intervals in PWC ASTRO and MWC S-R coincide with sustained ΔLP values exceeding 10,000 km (periods of lower entropy). Conversely, non-significant periods show more frequent low or intermittent ΔLP values. Notably, between 2021 and 2024, ΔLP values were high and increasing, exhibiting a lag of 10 to 12 months.

While the moderating role of the atmosphere and oceans is fundamental, ΔLP oscillations appear to configure significant coupling periods. This dynamics predisposes conditions for climate extremes and phase-shifts in phenomena such as ENSO (e.g., the "Triple-Dip" La Niña 2020–2023), altering pressure centers and precipitation distribution, as evidenced by the "ice and fire" events of early 2026. This approach is not deterministic but proposes a significant coherence based on information transfer and orbital kinematics.

4. Geodynamic Observation: The "Solsticialization" of Equinoxes

An additional descriptive consideration, consistent with the kinematic drift of ΔLP, is the gradual trend of the March and September equinoxes toward a geodynamic configuration that resembles "solstice-like behavior" rather than a theoretical perfect equinox. Although these changes appear subtle on solar scales, they represent significant shifts in Earth's energy distribution framework when scaled to planetary dimensions.

Empirical Evidence from CERES (2024 Record): Data from the **CERES TOA** incoming flux table confirms this trend, with 2024 marking a relevant tipping point. The months adjacent to the September equinox at **-45.5° S** reached the highest values in the entire 26-year series:

- **August:** 187.90 W/m² (Series maximum).
- **September:** 280.17 W/m² (Series maximum).
- **October:** 383.41 W/m² (Series maximum).

This "solsticialization" suggests that increased energy coupling in adjacent months during periods of high S-R Synergy pushes the system into new energetic states. This is not necessarily a smooth transition; empirically, many ENSO phases (El Niño/La Niña) initiate or strengthen around the September equinox and undergo phase-shifts near March.

This trend is not restricted to the Southern Hemisphere; CERES data for the Northern Hemisphere (+45.5° N) in 2024 also established a triple record for the March equinox window: March (294.83 W/m²), April (386.77 W/m²), and May (453.78 W/m²); all reached their absolute historical maximums within the CERES series. This parallel behavior with the September records in the Southern Hemisphere confirms the peak in ΔLP synergy (2021–2024).

This solsticialization is presented constantly by declination, but appears significantly in radiation and climate indices during periods of coupling and/or synergies, demonstrating the complexity of the dynamics through significant periods of low entropy in the data (higher coherence, for example).

Coherence and Persistence

The high statistical coherence found in our PWC/MWC analysis aligns with these empirical records. This suggests that orbital kinematic states (ΔLP) precondition the synchronization and intensity of these oscillatory climate events through significant periods of synergy between the astronomical variable and net radiation.

A clear example of this is the recent synergy period initiated between 2020 and 2022, which shows no clear signs of interruption and leaves open the question of whether it could be prolonged, similar to the "purely astronomical" period of 2004–2012 (PWC lag 4 to 10), which maintained high coherence with sustained high ΔLP values and only one low

ΔLP value in the entire sub-series. These results are not presented as a deterministic proof, but as a significant and coherent association that deserves further investigation.

TABLES

TABLE 1. Master Astronomical Dataset: September Equinox Kinematic Series (2000-2025)

Year	Deg	Min	Sec	Decl_Dec	Distance_ua	LatProj_AU	LP KM	Delta_LP KM
2000	0	0.0	11.364	0.00316	1.0034954403	0.000055277075	8269	+0
2001	0	0.0	19.102	0.00530	1.0034890839	0.000092898175	13897	+5628
2002	0	0.0	40.784	0.01133	1.0034556370	0.000198395086	29679	+15782
2003	0	1.0	6.241	0.01840	1.0035210213	0.000322251859	48208	+18529
2004	0	1.0	21.205	0.02256	1.0034581238	0.000395034919	59096	+10888
2005	0	1.0	48.252	0.03007	1.0034546587	0.000526633558	78783	+19687
2006	0	2.0	2.521	0.03403	1.0035457601	0.000596075520	89172	+10389
2007	0	2.0	23.812	0.03995	1.0035051237	0.000699634847	104664	+15492
2008	0	2.0	50.364	0.04732	1.0035293325	0.000828858065	123995	+19332
2009	0	2.0	57.432	0.04929	1.0035397645	0.000863230270	129137	+5142
2010	0	3.0	20.803	0.05578	1.0034966610	0.000976900007	146142	+17005
2011	0	3.0	46.091	0.06280	1.0035635465	0.001100040551	164564	+18422
2012	0	4.0	1.192	0.06700	1.0035281871	0.001173423111	175542	+10978
2013	0	4.0	26.195	0.07394	1.0035029572	0.001295057024	193738	+18196
2014	0	4.0	40.312	0.07787	1.0035834094	0.001363873464	204033	+10295
2015	0	5.0	1.621	0.08378	1.0035266610	0.001467457846	219529	+15496
2016	0	5.0	30.504	0.09180	1.0035206983	0.001607931774	240543	+21015
2017	0	5.0	41.232	0.09479	1.0035555204	0.001660223620	248366	+7823
2018	0	6.0	2.134	0.10059	1.0035323731	0.001761866727	263572	+15206
2019	0	6.0	29.071	0.10807	1.0036012399	0.001893053438	283197	+19625
2020	0	6.0	40.825	0.11134	1.0035904943	0.001950208559	291747	+8550
2021	0	7.0	2.582	0.11738	1.0035501402	0.002055980937	307570	+15823
2022	0	7.0	19.991	0.12222	1.0036361286	0.002140900544	320274	+12704
2023	0	7.0	38.324	0.12731	1.0036038239	0.002229987375	333601	+13327
2024	0	8.0	5.682	0.13491	1.0035853090	0.002363062104	353509	+19908
2025	0	8.0	15.312	0.13759	1.0036236121	0.002410029819	360535	+7026

TABLE 2. Master Astronomical Dataset: March Equinox Kinematic Series (2000-2025)

Year	Deg	Min	Sec	Decl_Dec	Distance_ua	LatProj_AU	LP KM	Delta_LP KM
2000	0	0.00	4.78	-0.00133	0.9959600545	-0.0000230901	-3454	+0
2001	0	0.00	21.46	-0.00596	0.9960346004	-0.0001036478	-15505	-12051
2002	0	0.00	37.42	-0.01039	0.9960096381	-0.0001806789	-27029	-11524
2003	0	0.00	51.56	-0.01432	0.9959504466	-0.0002489625	-37244	-10215
2004	0	1.00	13.76	-0.02049	0.9960030673	-0.0003561548	-53280	-16036
2005	0	1.00	30.55	-0.02515	0.9959780387	-0.0004372525	-65412	-12132
2006	0	1.00	56.95	-0.03249	0.9959569810	-0.0005646972	-84478	-19065
2007	0	2.00	11.19	-0.03644	0.9959844653	-0.0006334586	-94764	-10287
2008	0	2.00	25.06	-0.04029	0.9959388106	-0.0007004001	-104778	-10014
2009	0	2.00	53.17	-0.04810	0.9959684427	-0.0008361767	-125090	-20312
2010	0	3.00	13.13	-0.05365	0.9959490681	-0.0009325179	-139503	-14412
2011	0	3.00	33.86	-0.05941	0.9958855971	-0.0010325468	-154467	-14964
2012	0	3.00	57.08	-0.06586	0.9959627709	-0.0011447556	-171253	-16786
2013	0	4.00	14.16	-0.07060	0.9959640057	-0.0012272386	-183592	-12339
2014	0	4.00	38.09	-0.07725	0.9959147699	-0.0013426860	-200863	-17271
2015	0	4.00	55.27	-0.08202	0.9959470022	-0.0014257118	-213283	-12420
2016	0	5.00	9.71	-0.08603	0.9959065880	-0.0014953792	-223706	-10422
2017	0	5.00	36.01	-0.09334	0.9959360977	-0.0016223871	-242706	-19000
2018	0	5.00	51.78	-0.09772	0.9959536299	-0.0016985709	-254103	-11397
2019	0	6.00	3.53	-0.10098	0.9958742635	-0.0017551902	-262573	-8470
2020	0	6.00	25.99	-0.10722	0.9959189540	-0.0018637039	-278806	-16233
2021	0	6.00	44.66	-0.11241	0.9959060141	-0.0019538092	-292286	-13480
2022	0	7.00	12.79	-0.12022	0.9958232114	-0.0020894598	-312579	-20293
2023	0	7.00	36.16	-0.12671	0.9958748777	-0.0022024015	-329475	-16896
2024	0	7.00	50.46	-0.13068	0.9958642583	-0.0022714388	-339802	-10328
2025	0	8.00	19.55	-0.13876	0.9958887671	-0.0024119371	-360821	-21018

Note: As specified in the manuscript, the astronomical data originates from **NASA** time standards and ephemeris data from the **IMCCE (Paris Observatory)**.

TABLE 3. CERES TOA Incoming Solar Flux (45.5° S) EBAF Ed4.2 (2000-2025) W/m^2

Year	JAN	FEB	MAR	APR	MAY	JUN	JUL	AUG	SEP	OCT	NOV	DEC
2000	--	--	319.83	218.04	143.82	112.18	127.32	187.41	279.30	382.89	470.02	512.43
2001	492.24	420.60	320.74	218.72	144.29	112.27	127.05	186.74	278.46	381.99	469.34	512.26
2002	492.78	421.44	321.75	219.50	144.72	112.36	126.70	186.08	277.69	381.12	468.73	512.16
2003	493.00	422.04	322.40	220.17	145.11	112.37	126.40	185.46	276.86	380.00	468.07	511.85
2004	493.17	420.99	319.71	217.87	143.73	112.15	127.28	187.34	279.34	382.71	469.78	512.13
2005	491.77	420.20	320.51	218.56	144.13	112.19	127.00	186.74	278.48	381.88	469.15	511.90
2006	492.21	420.93	321.35	219.29	144.61	112.28	126.70	186.07	277.66	381.02	468.51	511.72
2007	492.57	421.63	322.21	220.02	145.01	112.35	126.40	185.46	276.81	380.18	467.99	511.64
2008	493.00	420.78	319.51	217.71	143.64	112.11	127.32	187.40	279.33	382.66	469.70	511.95
2009	491.70	420.06	320.37	218.44	144.08	112.19	127.03	186.78	278.54	381.86	469.14	511.82
2010	492.11	420.87	321.29	219.23	144.55	112.28	126.76	186.20	277.77	381.10	468.65	511.77
2011	492.58	421.62	322.15	220.02	145.02	112.37	126.47	185.58	276.96	380.39	468.25	511.89
2012	493.14	420.88	319.53	217.72	143.64	112.15	127.40	187.58	279.60	382.93	469.98	512.17
2013	491.80	420.11	320.39	218.42	144.09	112.24	127.15	186.97	278.81	382.09	469.36	512.10
2014	492.21	420.79	321.38	219.24	144.55	112.31	126.85	186.36	277.98	381.26	468.92	512.02
2015	492.79	421.86	322.25	220.01	144.99	112.39	126.57	185.70	277.11	380.56	468.35	511.87
2016	493.10	420.82	319.47	217.59	143.58	112.15	127.45	187.62	279.63	382.95	469.94	512.04
2017	491.69	419.96	320.22	218.31	144.01	112.20	127.14	186.97	278.75	382.14	469.35	511.91
2018	492.05	420.64	321.05	219.04	144.44	112.27	126.84	186.35	277.95	381.29	468.75	511.80
2019	492.48	421.43	321.93	219.75	144.86	112.33	126.54	185.71	277.12	380.46	468.19	511.70
2020	492.90	420.58	319.26	217.47	143.50	112.12	127.47	187.68	279.68	382.99	469.94	512.11
2021	491.71	419.93	320.18	218.25	143.96	112.21	127.21	187.11	278.93	382.27	469.49	512.09
2022	492.26	420.89	321.20	219.12	144.50	112.36	126.97	186.55	278.26	381.68	469.15	512.08
2023	492.80	421.77	322.23	219.95	144.94	112.45	126.68	186.00	277.54	381.06	468.76	512.21
2024	493.37	420.83	319.50	217.64	143.59	112.24	127.66	187.90	280.17	383.41	470.44	512.57
2025	492.09	420.19	320.43	218.37	144.01	112.30	127.36	187.31	279.21	382.58	469.86	512.23

TABLE 4. CERES TOA Incoming Solar Flux (+45.5° N) EBAF Ed4.2 (2000-2025) W/m^2

Year	JAN	FEB	MAR	APR	MAY	JUN	JUL	AUG	SEP	OCT	NOV	DEC
2000	--	--	293.96	385.94	453.16	481.51	464.67	406.78	322.12	229.53	154.02	120.01
2001	139.18	203.26	293.21	385.23	452.89	481.52	465.11	407.25	322.80	230.19	154.43	120.06
2002	138.86	202.64	292.61	384.66	452.48	481.54	465.19	407.75	323.57	230.84	154.88	120.14
2003	138.46	201.90	291.65	383.88	451.94	481.22	465.45	408.31	324.29	231.39	155.32	120.17
2004	138.04	202.60	294.04	385.92	453.10	481.34	464.34	406.36	321.93	229.29	153.86	119.93
2005	139.11	203.20	293.22	385.19	452.63	481.23	464.69	406.97	322.59	229.96	154.31	119.97
2006	138.77	202.53	292.44	384.53	452.34	481.24	464.99	407.47	323.32	230.63	154.74	120.03
2007	138.39	201.84	291.68	383.85	451.84	481.13	465.24	408.05	324.00	231.31	155.22	120.12
2008	138.05	202.63	294.05	385.90	453.06	481.23	464.27	406.20	321.69	229.10	153.76	119.89
2009	139.16	203.26	293.28	385.23	452.69	481.22	464.61	406.81	322.44	229.80	154.23	119.95
2010	138.80	202.63	292.57	384.68	452.38	481.26	465.00	407.46	323.23	230.53	154.71	120.03
2011	138.46	201.96	291.82	384.10	452.09	481.30	465.31	408.03	323.97	231.29	155.23	120.17
2012	138.15	202.81	294.27	386.15	453.28	481.44	464.33	406.33	321.79	229.11	153.78	119.93
2013	139.25	203.42	293.50	385.44	452.94	481.47	464.83	406.95	322.54	229.80	154.22	120.01
2014	138.89	202.73	292.86	384.94	452.62	481.44	465.08	407.56	323.25	230.50	154.73	120.09
2015	138.58	202.20	292.09	384.33	452.25	481.39	465.46	408.04	323.92	231.24	155.18	120.15
2016	138.21	202.91	294.40	386.17	453.31	481.42	464.32	406.16	321.59	228.98	153.70	119.90
2017	139.28	203.48	293.54	385.51	452.90	481.34	464.57	406.68	322.24	229.68	154.14	119.96
2018	138.90	202.77	292.76	384.83	452.49	481.27	464.88	407.25	322.99	230.34	154.59	120.03
2019	138.55	202.13	292.01	384.15	452.05	481.18	465.14	407.79	323.70	231.04	155.06	120.11
2020	138.21	202.92	294.41	386.21	453.29	481.32	464.19	406.02	321.44	228.86	153.63	119.91
2021	139.35	203.59	293.71	385.64	452.98	481.40	464.63	406.69	322.23	229.61	154.12	120.00
2022	139.02	203.03	293.08	385.23	452.91	481.67	465.15	407.43	323.14	230.44	154.65	120.10
2023	138.71	202.41	292.47	384.73	452.52	481.71	465.44	408.14	323.96	231.25	155.17	120.22
2024	138.40	203.17	294.83	386.77	453.78	481.83	464.68	406.20	321.78	228.95	153.71	120.01
2025	139.52	203.85	294.13	386.12	453.39	481.80	464.97	406.89	322.33	229.64	154.16	120.02

TABLE 5. BEST INDEX (BIVARIATE ENSO STATE) SERIES: 2000-2025

Year	JAN	FEB	MAR	APR	MAY	JUN	JUL	AUG	SEP	OCT	NOV	DEC
2000	--	--	-1.20	-1.06	-0.66	-0.39	-0.16	-0.43	-0.61	-0.74	-1.32	-0.67
2001	-0.81	-0.97	-0.46	-0.12	0.31	0.00	0.32	0.41	-0.17	0.06	-0.44	0.33
2002	-0.15	-0.34	0.49	0.37	0.96	0.94	0.93	1.23	0.96	1.01	1.05	1.35
2003	0.74	0.91	0.79	0.23	0.01	0.29	0.15	0.18	0.24	0.42	0.43	-0.20
2004	0.88	-0.33	0.08	0.64	-0.22	0.65	0.80	0.86	0.73	0.58	0.79	0.88
2005	0.25	1.87	0.35	0.72	1.03	0.23	0.12	0.33	-0.14	-0.54	-0.04	-0.22
2006	-1.14	-0.32	-0.98	-0.51	0.47	0.40	0.52	0.99	0.82	1.21	0.50	0.83
2007	0.82	0.31	0.12	0.11	0.02	-0.15	0.06	-0.43	-0.69	-1.06	-1.21	-1.45
2008	-1.59	-2.10	-1.18	-0.90	-0.27	-0.45	-0.01	-0.37	-0.75	-0.72	-0.88	-0.98
2009	-1.19	-1.64	-0.36	-0.54	0.66	0.68	0.59	0.95	0.30	1.77	1.44	1.67
2010	1.53	1.72	1.25	-0.18	-0.75	-0.70	-2.02	-2.29	-2.57	-2.21	-1.79	-2.66
2011	-2.30	-2.58	-2.22	-1.71	-0.63	-0.31	-0.82	-0.79	-1.15	-1.04	-1.40	-2.09
2012	-1.11	-0.67	-0.73	-0.01	-0.06	0.43	0.52	0.63	0.22	-0.06	0.01	0.41
2013	-0.09	-0.05	-0.98	-0.12	-0.76	-0.93	-0.71	-0.33	-0.18	-0.07	-0.55	0.83
2014	-1.08	-0.28	0.59	-0.16	0.09	0.38	0.36	0.64	0.87	0.75	1.22	0.83
2015	0.94	0.20	0.86	0.91	1.69	1.53	2.30	2.45	2.63	2.53	1.75	1.72
2016	2.82	2.60	1.23	1.75	0.19	-0.27	-0.42	-0.87	-1.08	-0.24	-0.19	-0.38
2017	-0.22	0.05	-0.57	0.39	0.20	0.51	-0.31	-0.51	-0.71	-0.93	-1.12	-0.27
2018	-1.07	-0.08	-1.35	-0.51	-0.26	0.25	0.15	0.27	0.96	0.25	0.60	-0.11
2019	0.38	1.34	0.83	0.59	1.05	0.91	0.76	0.25	1.01	0.62	1.10	0.70
2020	0.30	0.36	0.41	0.41	-0.32	0.10	-0.24	-1.09	-0.99	-1.02	-1.01	-1.61
2021	-1.72	-1.56	-0.66	-0.59	-0.62	-0.23	-1.12	-0.70	-0.81	-0.96	-1.19	-1.46
2022	-0.63	-1.12	-1.62	-1.73	-1.98	-1.61	-0.95	-1.45	-1.79	-1.78	-0.60	-1.75
2023	-1.23	-1.29	-0.13	0.14	1.44	0.77	1.29	1.77	2.12	1.29	1.70	1.15
2024	0.65	1.85	0.62	1.01	0.10	0.27	0.85	-0.63	0.11	-0.47	-0.38	-0.97
2025	-0.43	-0.58	-0.96	-0.31	-0.27	-0.10	-0.37	-0.38	-0.51*	-1.21*	-0.95*	-0.97*

CLARIFICATION: SEPTEMBER TO DECEMBER 2025 VALUES (MARKED WITH *) WERE CALCULATED

Summary Technical Notes

1. Data Provenance & Astronomical Alignment.

All astronomical datasets, NASA time standards, and ephemeris data used in this manuscript originate from **NASA** and the **IMCCE (Paris Observatory)**, respectively. This ensures kinematic precision for equinox and solar flux positioning. Refer to the manuscript for specific orbital parameterizations.

2. Incoming Solar Flux Data (CERES EBAF Ed4.2)

Data Origin and Sources Incident solar radiation data at the Top of the Atmosphere (TOA) is sourced from NASA's **CERES** (Clouds and the Earth's Radiant Energy System) project.

- **Official Source:** CERES EBAF-TOA Ed4.2 Data Tool
- **Parameters:** TOA Fluxes and Solar Flux (Zonal Mean).
- **Time Range:** March 2000 to December 2025.
- **Astronomical Context:** As noted in the manuscript, these records are aligned with **NASA** time standards and ephemeris data from the **IMCCE (Paris Observatory)**.

Dataset Specifications Historical and projected series were processed for specific latitudes (±45.5° N/S) to analyze incoming solar flux variability:

- **Latitude +45.5° N**
- **Latitude -45.5° S**

3. BEST Index Calculation (Sep-Dec 2025)

This note clarifies the methodology used to calculate the **BEST Index** (Bivariate ENSO State Index) for the period of **September to December 2024**, based on official NOAA/CPC data.

Primary Data Sources

- **SST 3.4 (CPC/NOAA):** ERSST.v5 Niño 3.4 Index
- **SOI (CPC/NOAA):** Southern Oscillation Index

Official Bivariate Formula

To ensure high technical accuracy, the index is calculated using the bivariate normalization of oceanic and atmospheric signals:

BEST = [(SST_Anomaly / σ_SST) - (SOI / σ_SOI)] × (Scale_Factor / 2)

Standardization Parameters (1981-2010 Climatology):

- **SST Deviation (σ):** 0.92
- **SOI Deviation (σ):** 1.62
- **Scale Factor:** 1.75 (Adjusted to normalize bivariate amplitude).

Step-by-Step Validation (September 2025 Example)

Using the official observed inputs for September:

- **Niño 3.4 SST Anomaly:** -0.48 (Cooling ocean)
- **SOI Index:** +0.10 (Neutral/Cooling atmosphere)

Calculation Process:

1. **Ocean Normalization:** -0.48 / 0.92 = **-0.521**

2. **Atmosphere Normalization:** +0.10 / 1.62 = **0.061**
3. **Signal Difference:** -0.521 - 0.061 = **-0.582** *(Note: SOI is subtracted because a positive SOI value indicates cooling, consistent with a negative SST).*
4. **Applying Scale Factor:** (-0.582 / 2) × 1.75 = **-0.509**

Final Result for September 2025: -0.51